

國立交通大學

電子工程學系 電子研究所碩士班

碩士論文

高介電係數閘極電晶體之負偏壓溫度不穩定性引
致臨界電壓改變量分佈之統計特性和模式

**Statistical Characterization and Modeling of NBTI Induced
 ΔV_t Distribution in High-k Gate Dielectric pMOSFETs**

研究生：李啟偉

指導教授：汪大暉 博士

中華民國 一〇二 年 七 月

高介電係數閘極電晶體之負偏壓溫度不穩定性引致
臨界電壓改變量分佈之統計特性和模式

**Statistical Characterization and Modeling of NBTI Induced
 ΔV_t Distribution in High-k Gate Dielectric pMOSFETs**

研究生：李啟偉

Student : Chi-Wei, Li

指導教授：汪大暉 博士

Advisor : Dr. Tahui Wang



Submitted to Department of Electronics Engineering and
Institute of Electronics

College of Electrical and Computer Engineering

National Chiao Tung University

in Partial Fulfillment of the Requirements

for the Degree of

Master of Science

in

Electronic Engineering

July 2013

Hsinchu, Taiwan, Republic of China.

中華民國 一〇二 年 七 月

高介電係數閘極電晶體之負偏壓溫度不穩定性引致臨界電壓改變量分佈之統計特性和模式

學生：李啟偉

指導教授：汪大暉 博士

國立交通大學 電子工程學系 電子研究所

摘要

在本篇論文中，我們針對元件中個別的單電荷產生，藉由統計性的方法，探討了在高介電係數奈米級閘極電晶體元件中，負偏壓溫度不穩定性引致臨界電壓改變量之分佈。我們量測大量小面積High-k元件之單電荷產生特徵時間及其造成之臨界電壓漂移。我們發現單電荷產生之特徵時間有數decade之廣。基於RD 模型之基礎，我們提出一個統計模型，結合實驗萃取之單電荷產生之特徵時間及單電荷造成之臨界電壓漂移分佈，成功地以蒙地卡羅模擬重現實驗數據之 ΔV_t 分佈及其和NBTI 操作時間的關係。

Statistical Characterization and Modeling of NBTI Induced ΔV_t Distribution in High-k Gate Dielectric pMOSFETs

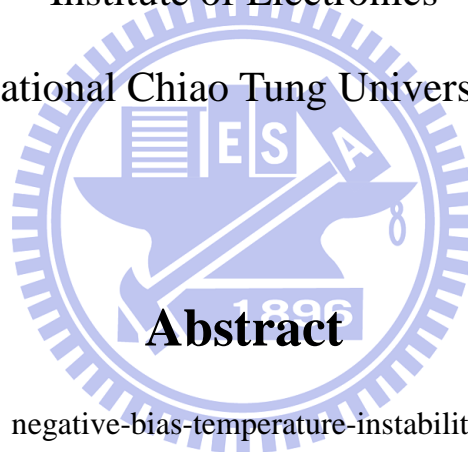
Student: Chi-Wei Li

Advisor: Dr. Tahui Wang

Department of Electronics Engineering &

Institute of Electronics

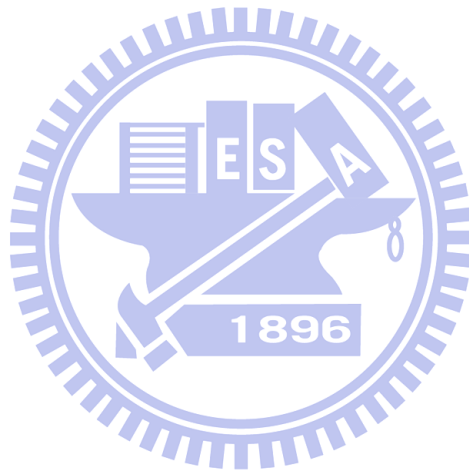
National Chiao Tung University



Abstract


In this thesis, a negative-bias-temperature-instability (NBTI) induced ΔV_t distribution is examined by a statistical study of individual trapped charge creations in nanoscale HfSiON gate dielectric pMOSFETs. We measure individual trapped charge creation times and corresponding threshold voltage shifts during NBTI stress in a large number of devices. The characteristic time distributions of the first three trapped charge creation are obtained. Wide dispersion of trap creation characteristic times in several decades is observed. A statistical model for an NBTI induced ΔV_t distribution by employing the RD model and convolving collected the trapped charge creation

times and a single trapped charge induced V_t shift is developed. Our model can reproduce measurement results of an overall NBTI induced ΔV_t distribution and its stress time evolutions well.



Acknowledgement

這篇論文之所以能夠完成，首先要感謝我的指導教授—汪大暉博士。在碩士生涯的兩年中，能向您學習十分幸運。在您嚴謹扎實的理論教導下，我學習到大量的新知識及正確的研究態度，謝謝您。我想我會永遠記得老師飛快的思考方式，還有發現新物理時眼睛一亮的表情，那種對研究的熱情，是會感染學生的。感謝老師的厚愛，使我參與了相當多篇論文的研究，其中老師對自己研究內容十分有信心的強悍，讓我學習到遇到困難只要相信自己，一定能打開一條活路。無論是老師的能力或是待人處事公私分明的態度，都是我在未來的人生中學習的目標，在此深表我對您的感謝。



感謝實驗室的學長與同學。感謝鍾岳庭學長，在大四下帶領我融入實驗室，教導我量測技術以及實驗原理，並且在我碩士生涯兩年間也時常幫助我，給我很多建議。感謝王明璋學長，在我升碩一的暑假教導我使用模擬軟體，感謝學長細心的教學，使我能快速上手。感謝謝泓達學長，在我碩一下到碩二上研究卡關的時候，以你自身的模擬經驗提點我，幫助我進入狀況。最後要感謝邱榮標學長，從碩一的暑假開始到現在，從學長身上學習到了很多經驗與知識，不管是模擬上的經驗或是實驗上鉅細靡遺的剖析能力，都讓我大開眼界。感謝學長總是用嚴謹又有邏輯的思考方式以及優越的表達能力，仔細的為我解惑，使我受益良多。再來要感謝實驗室的同學的陪伴，讓我兩年的研究生生活充滿樂趣。特別要感謝宇恆，碩二和你一起研究的時光很充實，祝你未來能很快地順利取得博士學位。

感謝交大電子系壘，在碩士班兩年的時光，能和各位夥伴一起為比賽專心付出是很熱血又值得回憶的事。感謝政銘、小龜、川嘉，在電子所繁忙的研究生生活中，能一起擠出時間打球，不只令我們強健體魄，每次比賽完的聚餐總是充滿笑

聲，更是釋放壓力的最好管道。

感謝碩士班兩年的室友：效瑜、凱俞、蕭景、川嘉。和各位在寢室的時光總是特別的快樂，兩年來很感謝你們的包容以及照顧，祝各位都能順利地畢業，未來一帆風順。

感謝好友小馬，謝謝妳常與我分享生活上的點滴，每次聊天都覺得很輕鬆，說說笑笑的紓解了很多壓力，祝福妳能順利完成自己的目標。感謝好友貞觀，謝謝妳在我碩一下和碩二下最低落的時候聽我碎念，能認識妳真的是件相當幸運的事，每次和妳談完總是充滿能量，很感恩。未來的路還很長，祝福妳能克服一切挑戰，生活順順利利，過的輕鬆自然快樂。

最後要感謝我的家人。感謝我的父母、大姐靜容、二姐佳慧以及那位 24 年來，為了在未來的日子裡讓我更加珍惜而尚未出現的女朋友。謝謝你們無私的付出，讓我能夠無後顧之憂的完成學業。感謝你們提供一個溫暖的家，讓我在疲憊的時候能有一個避風港。家人的愛和支持是我能完成碩士學位的最大動力，謝謝你們。

2013, July 寫於風城新竹

Contents

Chinese Abstract	<i>i</i>
English Abstract	<i>ii</i>
Acknowledgement	<i>iv</i>
Contents	<i>vi</i>
Figure Captions	<i>viii</i>
Chapter 1 Introduction	1
Chapter 2 Characterization of Individual NBTI	7
Trapped Charge Creation	
2.1 Preface	7
2.2 Device Details and Measurement Setup	8
2.3 Single Charge Induced ΔV_t Distribution and Percolation Effect	8
2.4 Characteristic Times for Trapped Charge Creation	10
Chapter 3 Modeling of an NBTI induced ΔV_t Distribution	21
3.1 Preface	21
3.2 Reaction-Diffusion Model (RD Model)	22
3.3 Relationship of τ_i Distributions in Trapped Charge Creation	23
3.4 NBTI Stress Induced ΔV_t Spread	23
3.5 Monte Carlo Simulation Results and Discussion	24
Chapter 4 Conclusion	37

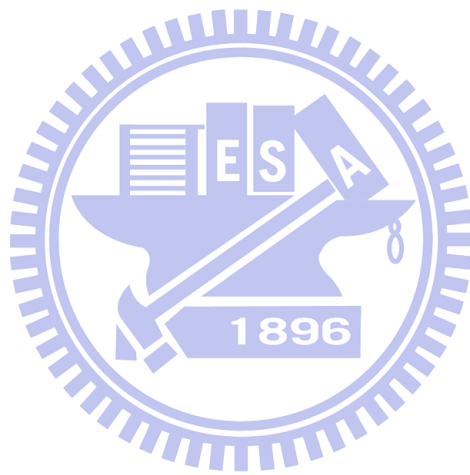


Figure Captions

Chapter 1

- Fig. 1.1** Absolute Static Noise Margin (SNM) change vs. threshold voltage shift (ΔV_t) for different V_{DD} , indicating that the SNM change increases as V_{DD} decreases. 4
- Fig. 1.2** Percentage frequency reduction of NBTI stressed ring oscillator versus supply voltage (V_{DD}). The magnitude of the frequency reduction increases as V_{DD} decreases. 5
- Fig. 1.3** Illustration of an NBTI induced ΔV_t distribution and a device qualification criterion. 6

Chapter 2

- Fig. 2.1** (a) Continuous V_t evolutions in NBTI stress and relaxation in a large-area ($W/L=3\mu\text{m}/2\mu\text{m}$) high-k pMOSFET. V_g is -1.8V in stress. $T=25^\circ\text{C}$. 11
- (b) Stepwise V_t evolutions in NBTI stress and relaxation in a small-area ($W/L=80\text{nm}/30\text{nm}$) high-k pMOSFET. V_g is -1.8V in stress. $T=25^\circ\text{C}$. The abrupt V_t shifts represent single-charge trapping and detrapping.
- Fig. 2.2** We characterize NBTI stress in high-k (HfSiON) gate dielectric and metal gate (TiN) MOSFETs. The devices have a gate length of 30nm, a gate width of 80nm and an equivalent oxide thickness of $\sim 1.0\text{nm}$. 12
- Fig. 2.3** (a) Schematic diagram for NBTI stress transient characterization. 13
- (b) The waveforms applied to the gate and the drain in stress and in

measurement phases.

Fig. 2.4 $\log(I_d)$ versus V_g plots before and after 100sec NBTI stress at $V_g = -1.8V$ in a pMOSFET. 14

Fig. 2.5 Example ΔI_d and V_t traces in NBTI stress. τ_1 , τ_2 and τ_3 are the 1st, 15
the 2nd and the 3rd trapped hole creation times, respectively. $\Delta v_{t,i}$ ($i = 1, 2, 3$) represents a single trapped hole creation induced threshold voltage shift.

Fig. 2.6 Illustration of channel surface potential and current pattern. When 16
the trapped charge locates on the main current path, it will induce larger Δv_t amplitude.

Fig. 2.7 The magnitude distributions of single-charge induced Δv_t collected 17
from NBTI stress and recovery V_t traces in 130 pMOSFETs. The solid line is drawn as a reference.

Fig. 2.8 The probability density distribution of a trapped charge (hole) 18
creation time in NBTI stress. τ_1 , τ_2 , and τ_3 are the 1st, the 2nd, and the 3rd trapped hole creation times, respectively, in a device. The three $\log(\tau)$ distributions have a similar shape but are shifted by an amount $n\log(i)$.

Fig. 2.9 We calculate the mean ($\langle \log(\tau_i) \rangle$) of the three $\log(\tau_i)$ distributions 19
and reveal a relationship $\langle \log(\tau_i) \rangle - \langle \log(\tau_1) \rangle \sim n\log(i)$. i is a sequence number in trapped charge creation in NBTI stress and n is about 5.6.

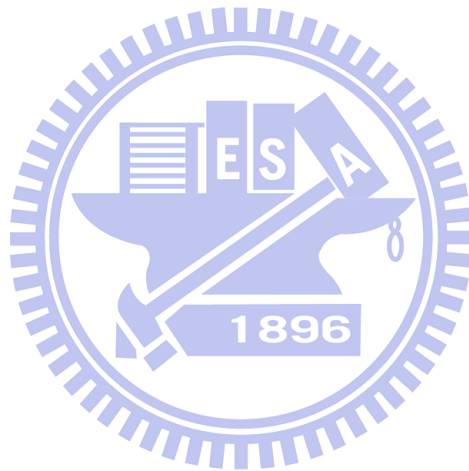
Table I The mean ($\langle \log(\tau_i) \rangle$) and the standard deviation of the three $\log(\tau_i)$ 20
distributions. i is a sequence number in trapped charge creation in NBTI stress.

Chapter 3

- Fig. 3.1** The probability density distributions of $\log(\tau_i) - n\log(i)$. The solid line represents a Gaussian-distribution fit. 27
- Fig. 3.2** NBTI induced ΔV_t versus number of created trapped holes in a device at a stress time of 0.01s (a), 1s (b) and 100s (c). Each data point represents a device. A straight line with a slope of 3.3 mV is drawn as a reference. 28
- Fig. 3.3** The mean of the ΔV_t distribution versus NBTI stress time from measurement and from our model. 29
- Fig. 3.4** The variance of the ΔV_t distribution versus NBTI stress time from measurement and from our model. 30
- Fig. 3.5** A Monte Carlo simulation flowchart. M is the number of precursors in a device. A precursor density of $1 \times 10^{12} \text{ 1/cm}^2$ is assumed. 31
- Fig. 3.6** Probability density distributions of a trapped charge (hole) creation time in a $\log(\tau)$ scale. The symbols are measurement result and the solid lines are from Monte Carlo simulation. 32
- Fig. 3.7** Complementary cumulative distribution functions (1-CDF) of NBTI induced ΔV_t from measurement and from a Monte Carlo simulation. The stress time is 0.01s (a), 1s (b) and 100s (c), respectively. The inset shows the probability distributions of ΔV_t . 33
- Fig. 3.8** Comparison of NBTI induced ΔV_t distributions (1-CDF) calculated from this model and from the Poisson distributed trap number model. The dots are measurement result. The stress time is 100 s. 34
- Fig. 3.9** The probability density distributions of a trapped charge number 35

from our model and from the Poisson distributed trap number model.

Table II NBTI failure rates in 100s stress based on two ΔV_t failure criteria. 36



Chapter 1

Introduction

The aggressive CMOS scaling has been reaching the physical limit of conventional SiO₂ MOSFETs as a result of significant direct tunneling current through ultrathin oxides. High-permittivity (high-k) gate dielectrics have emerged as a post-SiO₂ solution. Negative bias temperature instability (NBTI) has been recognized as a major concern in scaled high-permittivity (high-k) gate dielectric p-type metal-oxide-semiconductor field effect transistors (pMOSFETs) because of its significant impact on circuit performance and reliability [1-3]. The use of high-k gate dielectrics even expedites NBTI degradation [4-5]. NBTI caused noise margin degradation in SRAM cell (Fig. 1.1) and frequency degradation in a ring oscillator (Fig. 1.2) have been reported recently [6-7]. NBTI severity aggravates as supply voltage reduces in device scaling. In addition to digital circuits, NBTI is of particular importance for analog applications where the ability to match device characteristics to a high precision is critical [8]. For instance, in digital-to-analog converters, NBTI can pose a serious reliability issue as a small V_t shift in bias current source can cause large gain errors [9]. Therefore, it is important to carefully characterize the time evolution of threshold voltage to ensure the long-term viability of an integrated circuit.

As MOSFET reduce to a nanometer scale, the threshold voltage degradation due to NBTI varies considerably from one transistor to another. Two NBTI degradation models, a reaction-diffusion (RD) model [10] and a charge trapping model [11-12], have been proposed. In our earlier work [11], we reported that NBTI induced V_t

degradation exhibits two stages. The first stage is ascribed to the charging of pre-existing high-k traps and exhibits a $\log(t)$ dependence. The second stage is caused by high-k trap creation and follows power-law dependence on stress time. Since in this work our measured NBTI induced V_t degradation obeys a $t^{1/n}$ dependence ($n \sim 5.6$), an NBTI V_t distribution model will be developed based on the RD model.

The mean of an NBTI ΔV_t distribution, or a ΔV_t in a large-area device, can be well predicted by the RD model [10, 13-15], but the RD model alone is insufficient to describe an entire ΔV_t distribution in nanoscale transistors. In NBTI qualification, since it is the tail part of a ΔV_t distribution to determine a qualification pass/failure (Fig. 1.3), an accurate model of an overall ΔV_t distribution and its stress time evolutions is urgently needed in an NBTI qualification method.

In Chapter 2, we characterize NBTI trap creation and V_t shifts in small-area devices. Unlike a large-area device, NBTI induced V_t degradation proceeds in discrete steps in small-area devices [3, 16]. Due to the discrete nature of a V_t evolution, we are able to measure individual trapped charge creation times and each trapped charge induced V_t shift. A total V_t shift in an NBTI stressed device can be expressed as the sum of each individual trapped charge induced Δv_t , i.e., $\Delta V_t = \sum_{i=1}^N \Delta v_{t,i}$, where N is a total number of stress created traps in a device and Δv_t denotes a single trapped charge caused V_t shift. Two factors influence a ΔV_t distribution. One is the dispersion of Δv_t and the other is fluctuations in number of traps N in stressed devices. Single trapped charge (hole) induced Δv_t and its trapped charge (hole) creation time in NBTI stress are extracted from the measurement data.

In Chapter 3, we obtain the trapped charge (hole) creation time (τ_i) distributions

are Gaussian-like distributions. Relationship of τ_i distributions in trapped charge creation are derived by the RD model. A Monte Carlo model employing the RD model, collected the trapped charge creation time distributions and single trapped charge (hole) induced Δv_t distribution will be developed to simulate an NBTI induced ΔV_t distribution and its stress time evolutions. The mean and variance of ΔV_t are acquired during NBTI stress. In literature, a Poisson distributed trap number was usually assumed [17-19] in an NBTI stressed device to model a ΔV_t distribution. We also compare our model with Poisson model. However, the Poisson model based on a notion that individual trapped charge creations during NBTI stress are independent. In other words, each new trap creation in a device has the same probability regardless of how many traps have been created. Nevertheless, the RD model and measurement result show that NBTI degradation obeys a power-law dependence on stress time, implying that a new trap creation rate decreases with an increasing trapped charge number. Therefore, the use of a Poisson distribution model is contradictory to a measurement result and may exaggerate an NBTI induced ΔV_t distribution tail. Finally, we give a conclusion in Chapter 4.

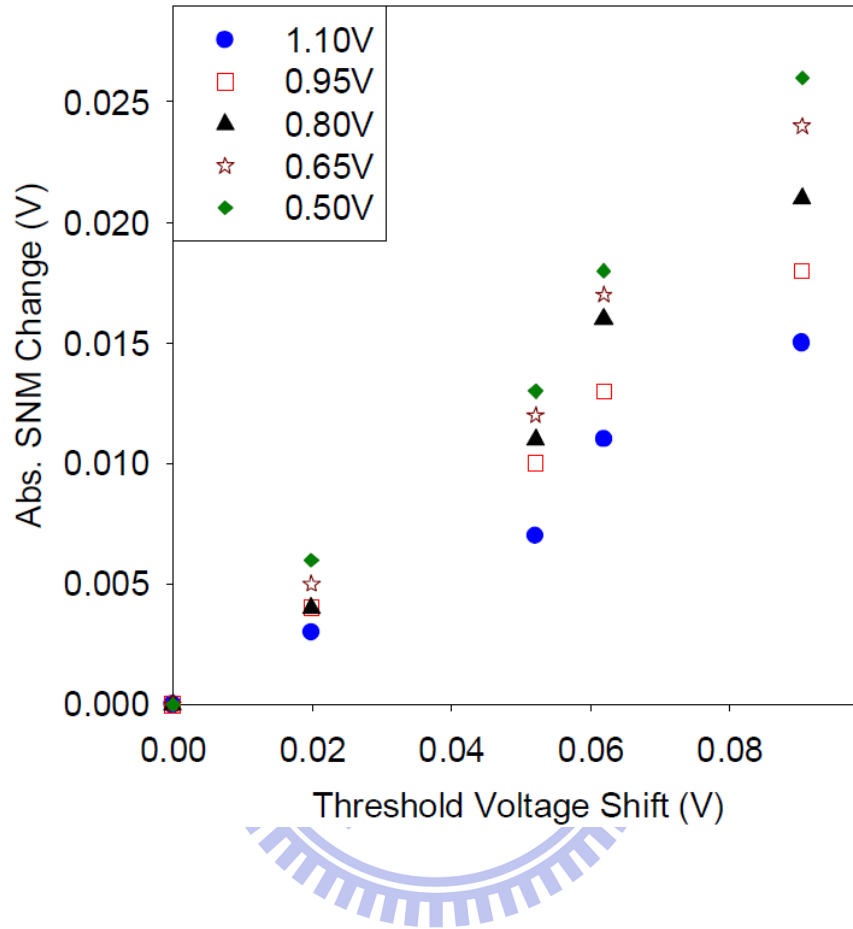


Fig. 1.1 Absolute Static Noise Margin (SNM) change vs. threshold voltage shift (ΔV_t) for different V_{DD} , indicating that the SNM change increases as V_{DD} decreases.

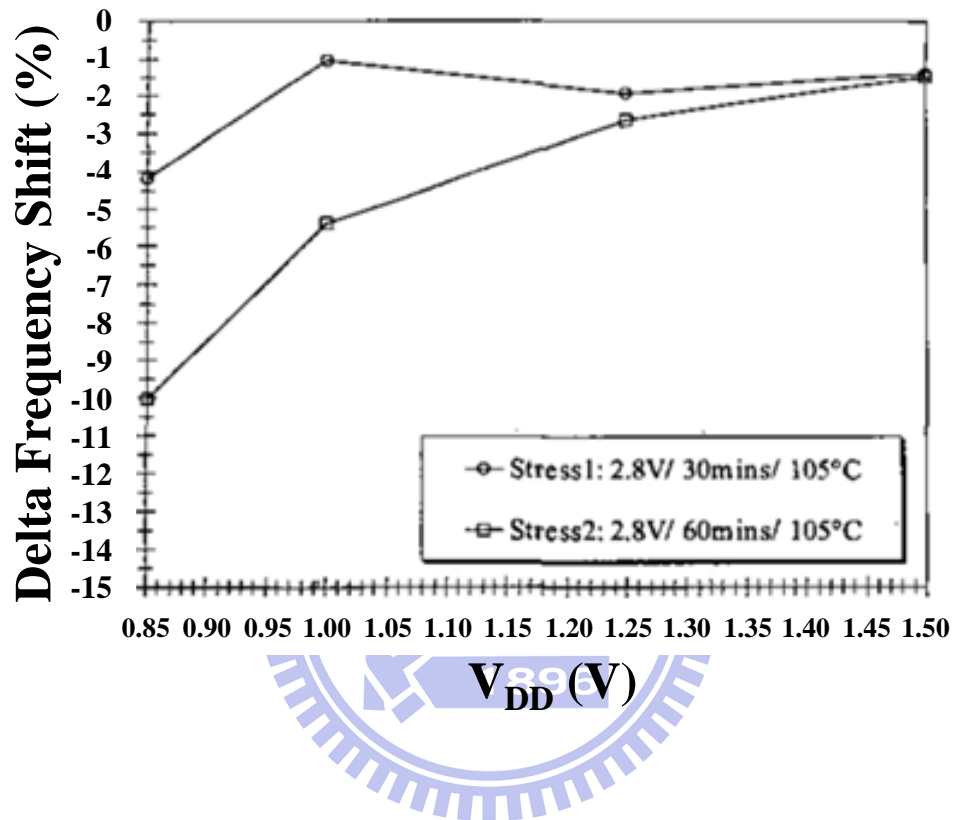


Fig. 1.2 Percentage frequency reduction of NBTI stressed ring oscillator versus supply voltage (V_{DD}). The magnitude of the frequency reduction increases as V_{DD} decreases.

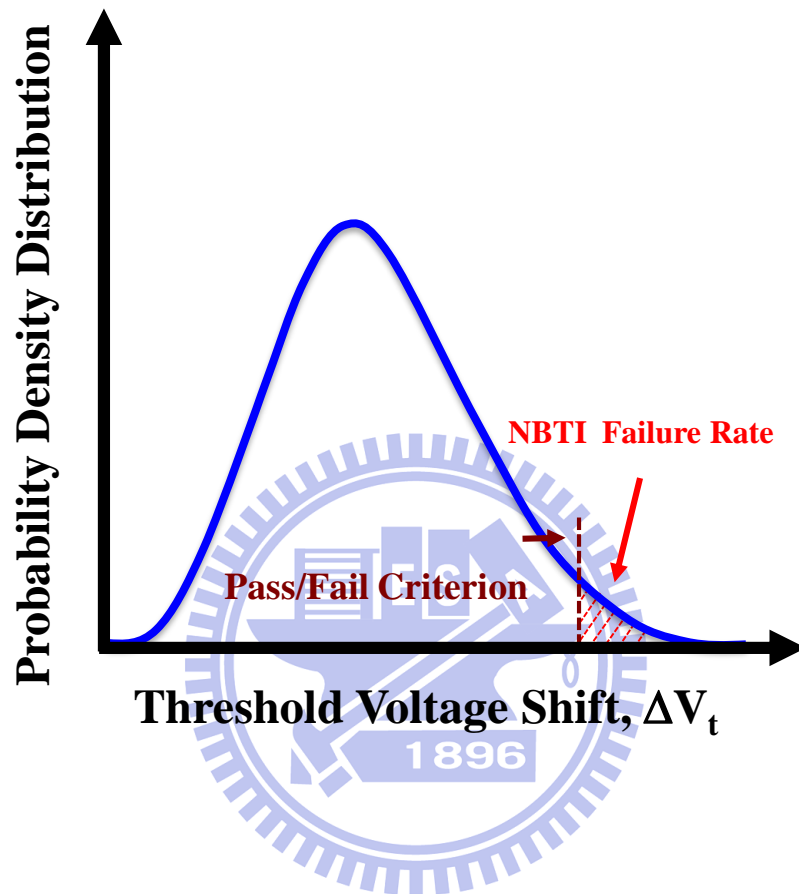


Fig. 1.3 Illustration of an NBTI induced ΔV_t distribution and a device qualification criterion.

Chapter 2

Characterization of Individual NBTI Trapped Charge Creation

2.1 Preface

As device dimensions reduce to a nanometer scale, NBTI induced V_t shifts scatter widely from a device to a device. Modeling of an entire NBTI induced ΔV_t distribution is needed to ensure that the tail of ΔV_t distribution does not cross the reliability criteria in a specified lifetime.

Conventionally, NBTI characterization is carried out by periodically interrupting stress to measure device electrical parameters such as V_t or drain current (I_d) degradation. Note that conventional measurement (for example, by Agilent 4156), which usually takes a few seconds between stress and recovery transitions, is unable to catch an initial transient in a μs to ms range and may significantly underestimate the magnitude of a transient effect. Owing to recent improvements in measurement techniques [20-22], a measurement delay can be reduced to μs (for example, by Agilent B1500) to avoid information missing during a switching transient.

In contrast to large-area devices (Fig. 2.1 (a)), we found that NBTI induced V_t degradation and recovery in nanoscale transistors proceed in discrete steps [22-26] due to augmentation of single charge effects in scaled devices. Example V_t evolutions in a small-area device ($W/L=80\text{nm}/30\text{nm}$) are shown in Fig. 2.1 (b). In the figure, each abrupt V_t change in stress/recovery V_t traces is caused by single charge

creation/detrapping in gate dielectrics. Due to the discrete nature of V_t evolutions, we are able to measure individual charge creation/detrapping times and the magnitudes of single charge induced V_t shifts. Statistical characterization of NBTI traps in nanoscale devices helps gain insight into mechanisms in NBTI stress.

2.2 Device Details and Measurement setup

We characterize NBTI stress in high-k (HfSiON) gate dielectric and metal gate (TiN) pMOSFETs. The devices have a gate length of 30nm, a gate width of 80nm and an equivalent oxide thickness (EOT) of ~1.0nm. The device structure we used in this thesis is illustrated in Fig. 2.2.

Schematic diagram for NBTI stress transient measurement is shown in Fig. 2.3 (a). The stress characterization scheme is similar to [27], i.e., in a stress-measurement-stress (SMS) sequence, as shown in Fig. 2.3 (b). In NBTI stress phase, $|V_{g, stress}|=1.8V$ and $V_d=0V$ at room temperature for 100sec. In measurement phase, the drain voltage $|V_{d, meas}|$ is 0.05V and the gate voltage $|V_{g, meas}|$ is chosen such that a pre-stress drain current is ~500nA. Drain current variations (ΔI_d) are recorded using Agilent B1500 with a switch delay time less than 1 μ s. A corresponding ΔV_t is obtained from a measured ΔI_d divided by a transconductance (g_m).

2.3 Single Charge Induced Δv_t Distribution and Percolation

Effect

To check on Si surface trap creation in NBTI stress, we monitor transconductance (g_m) and subthreshold swing (S) degradations during stress.

Pre-stress and post-stress subthreshold I_d - V_g are shown in Fig. 2.4. An almost parallel shift is noted, suggesting that V_t degradation is mainly caused by trapped charge creation in the bulk of gate dielectrics rather than surface traps. Both S and g_m degradations are less than 5% after the stress. For simplicity, a constant g_m is used when converting a ΔI_d into a ΔV_t . Fig. 2.5 shows example ΔI_d and V_t traces in NBTI stress. A small letter ($\Delta v_{t,i}$) denotes a single trapped hole creation induced V_t shift, where i denotes a trapped charge creation sequence number. A capital letter (ΔV_t) is a total V_t shift after stress.

In nanoscale MOSFETs, non-uniform 3D electrostatics and the discreteness and the randomness of substrate dopants determine current percolation paths in a channel (Fig. 2.6). Thus, each trapped charge creation has specific Δv_t amplitude depending on its position in a channel.

We measure and record the magnitudes of single-charge induced Δv_t in NBTI stress/recovery V_t traces in ~130 pMOSFETs. The magnitude distributions of the Δv_t are plotted in Fig. 2.7. The measurement resolution is about 1mV. Voltage steps with Δv_t less than 1mV are not recorded. The collected Δv_t from stress traces and from recovery traces have a similar distribution, characterized by an exponential function $f(|\Delta v_t|) = \exp(-|\Delta v_t|/\sigma_{amp})/\sigma_{amp}$ with a σ_{amp} of 3.3mV. A straight line with a slope of 3.3mV is drawn to serve as a reference. The exponential function is an empirical formula. The origin and the dispersion of the Δv_t have been studied thoroughly. In such small-area devices, single-charge induced Δv_t cannot be estimated from its distance to a gate electrode by using a 1D capacitance equation $C = \epsilon/d$ because of a strong random dopant induced current percolation effect (Fig. 2.6). The exponential

distribution is realized due to the percolation effect [3, 17-18, 28-29]. A 3D atomistic numerical device simulation shows a similar ΔV_t probability function [29].

2.4 Characteristic Times for Trapped Charge Creation

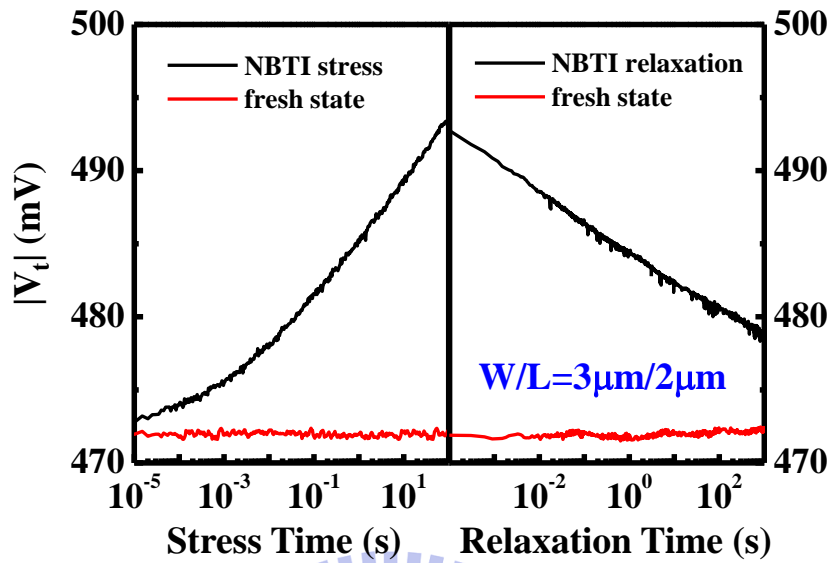
The second factor affecting an NBTI induced ΔV_t distribution is the dispersion of a characteristic time for a trapped hole creation. Individual trapped hole creation times are clearly defined in stress V_t traces, for example, τ_1 , τ_2 and τ_3 in Fig. 2.5. We collect the first three trapped hole creation times (τ_i , $i=1,2,3$) from about 130 devices. The probability density functions (PDFs) of the $\log(\tau_i)$, $i=1,2,3$, are shown in Fig. 2.8. It should be remarked that about 3% devices have less than 3 traps created in a stress period of 100sec. The mean ($\langle \log(\tau_i) \rangle$) and the standard deviation of the three $\log(\tau_i)$ distributions are indicated in Table I. The solid line in Fig. 2.8 is a fit by a Gaussian distribution.

$$f(\log(\tau)) = \frac{1}{\sqrt{2\pi}\sigma} \exp\left[-\frac{(\log(\tau) - \mu)^2}{2\sigma^2}\right] \quad \text{Eq. (2.1)}$$

The trap creation characteristic times scatter over several orders of magnitudes. The wide spread of τ_i is attributed to the dispersion from different local chemistry and 3D electrostatics such as random dopants and edge effects in a nanoscale device. We calculate the mean of each $\log(\tau_i)$ and reveal a relationship $\langle \log(\tau_i) \rangle - \langle \log(\tau_1) \rangle \sim n \log(i)$, as shown in Fig. 2.9. A statistical τ_i distribution model will be developed.

(a)

Large-Area Devices



(b)

Small-Area Devices

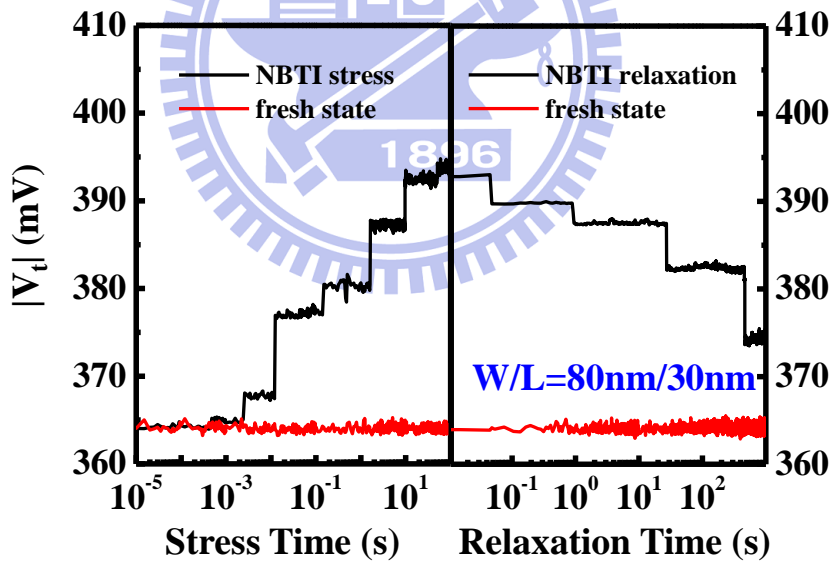


Fig. 2.1 (a) Continuous V_t evolutions in NBTI stress and relaxation in a large-area ($W/L=3\mu\text{m}/2\mu\text{m}$) high-k pMOSFET. V_g is -1.8V in stress. $T=25^\circ\text{C}$. (b) Stepwise V_t evolutions in NBTI stress and relaxation in a small-area ($W/L=80\text{nm}/30\text{nm}$) high-k pMOSFET. V_g is -1.8V in stress. $T=25^\circ\text{C}$. The abrupt V_t shifts represent single-charge trapping and detrapping.

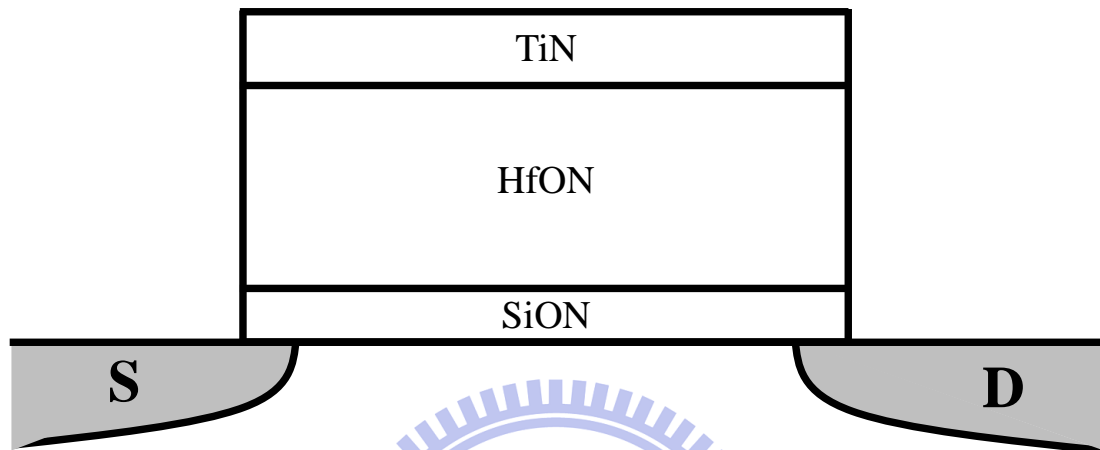
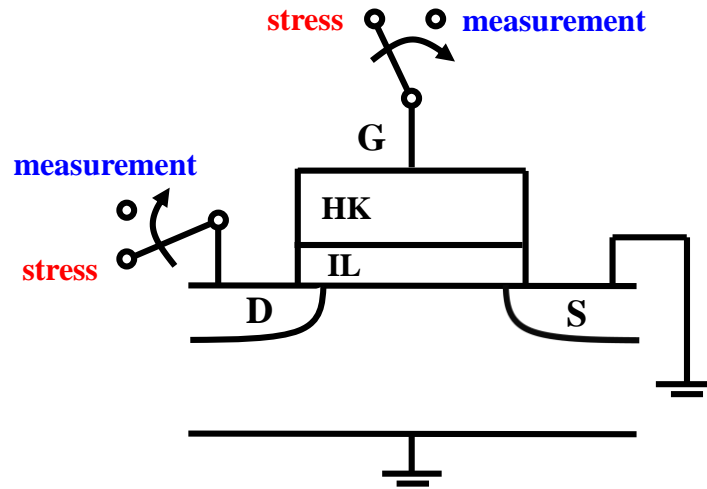


Fig. 2.2 We characterize NBTI stress in high-k (HfSiON) gate dielectric and metal gate (TiN) MOSFETs. The devices have a gate length of 30nm, a gate width of 80nm and an equivalent oxide thickness of ~1.0nm.

(a) Schematic diagram



(b) Waveforms of V_g and V_d

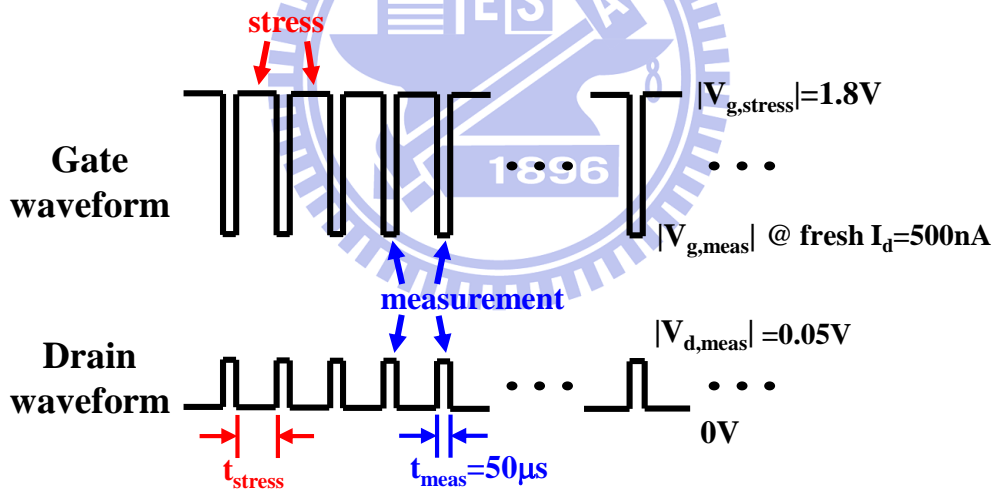


Fig. 2.3 (a) Schematic diagram for NBTI stress transient characterization. (b) The waveforms applied to the gate and the drain in stress and in measurement phases.

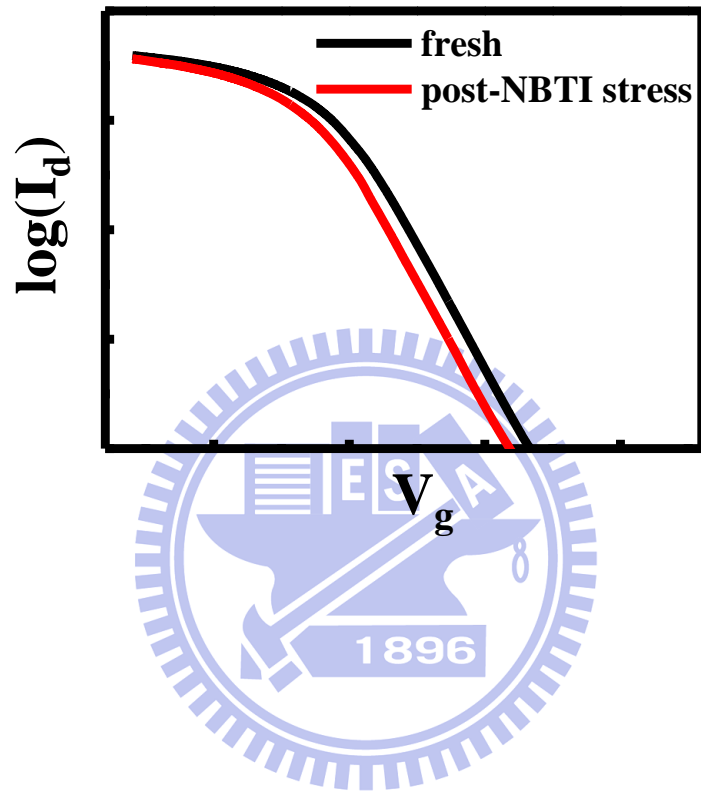


Fig. 2.4 $\log(I_d)$ versus V_g plots before and after 100sec NBTI stress at $V_g=-1.8V$ in a pMOSFET.

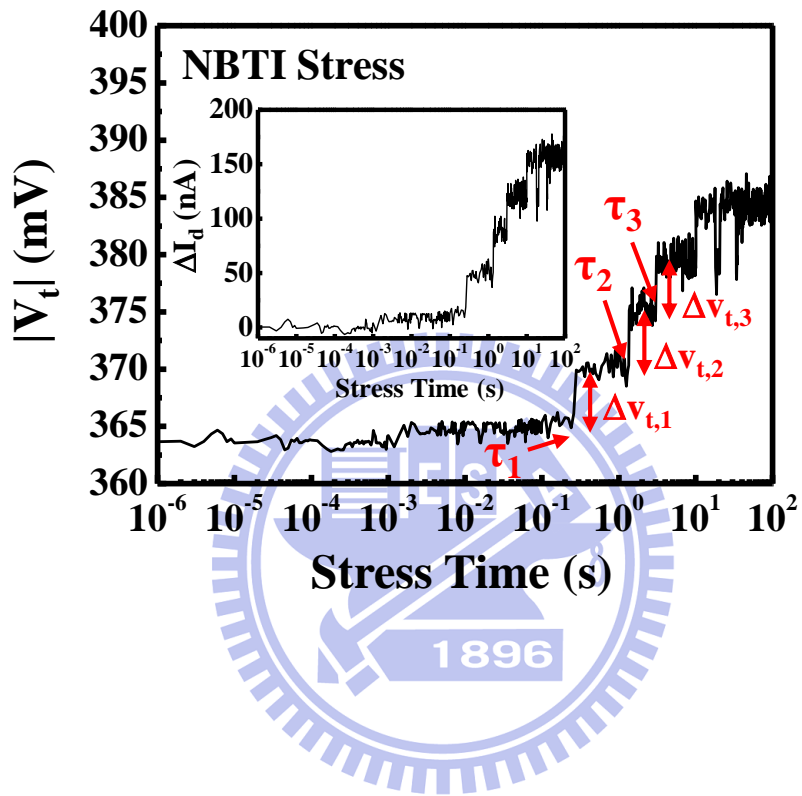


Fig. 2.5 Example ΔI_d and V_t traces in NBTI stress. τ_1 , τ_2 and τ_3 are the 1st, the 2nd and the 3rd trapped hole creation times, respectively. $\Delta v_{t,i}$ ($i = 1, 2, 3$) represents a single trapped hole creation induced threshold voltage shift.

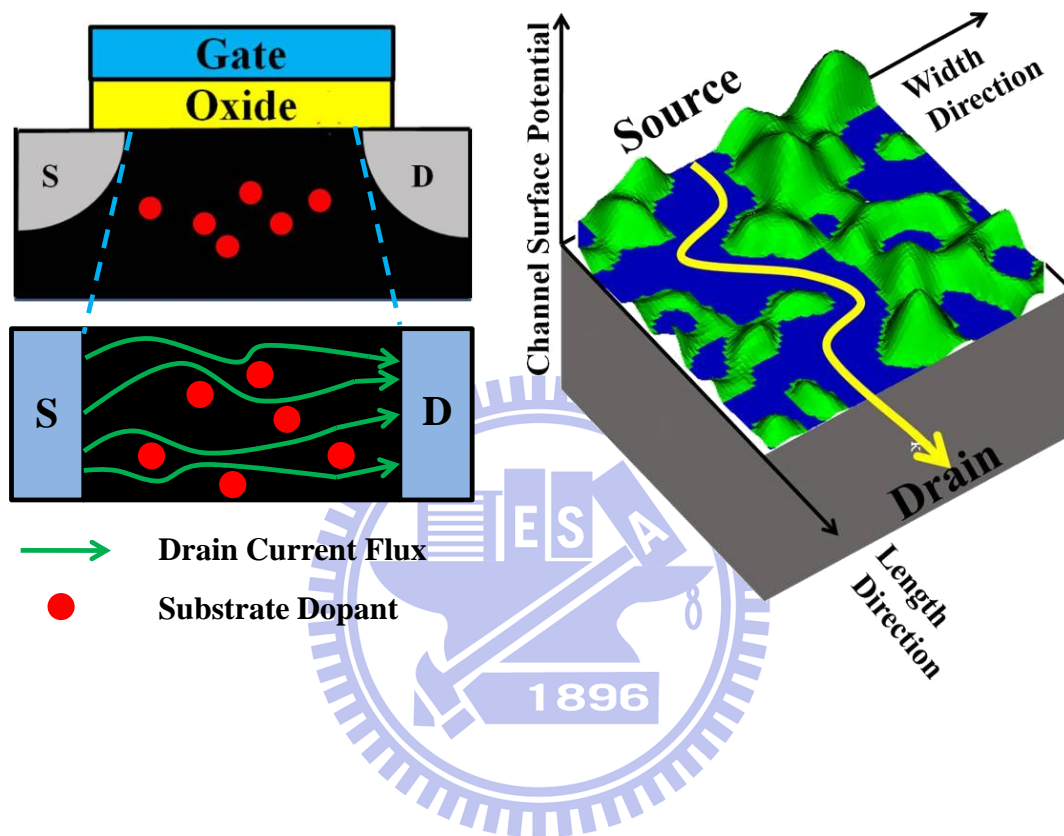


Fig. 2.6 Illustration of channel surface potential and current pattern. When the trapped charge locates on the main current path, it will induce larger Δv_t amplitude.

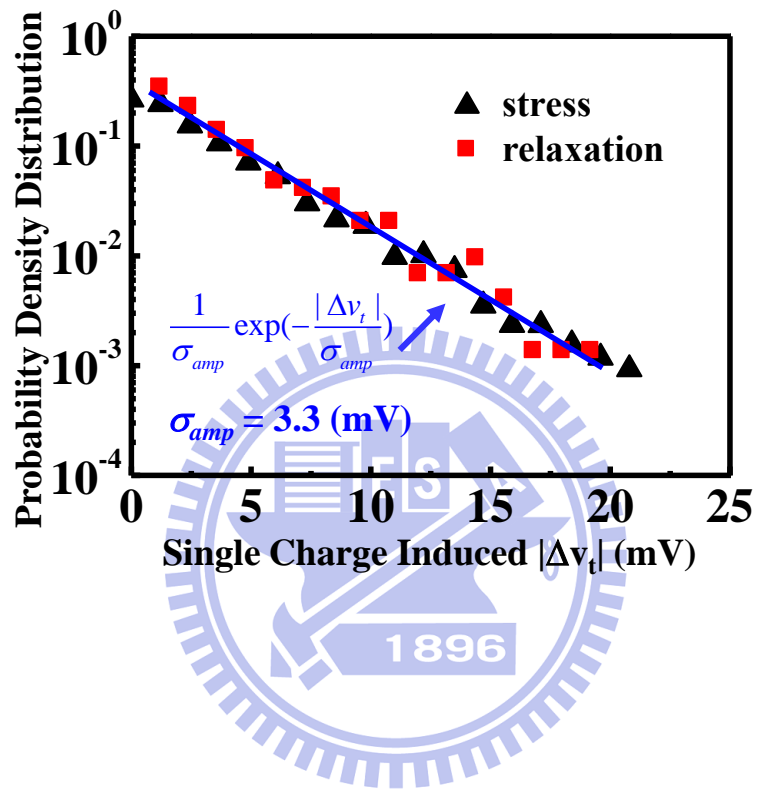


Fig. 2.7 The magnitude distributions of single-charge induced Δv_t collected from NBTI stress and recovery V_t traces in 130 pMOSFETs. The solid line is drawn as a reference.

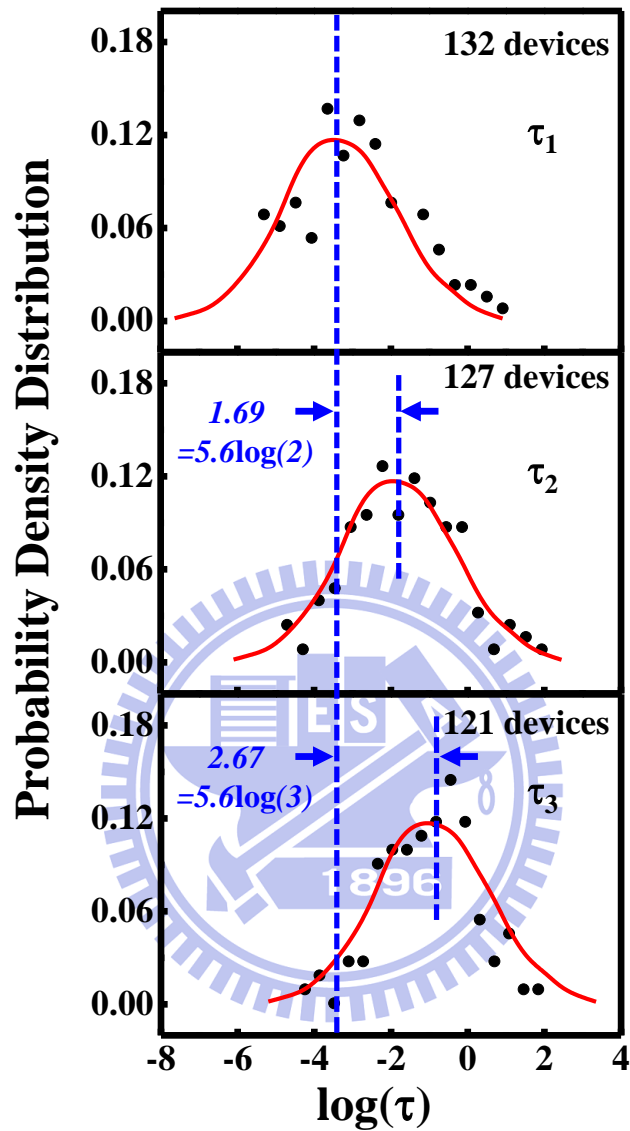


Fig. 2.8 The probability density distribution of a trapped charge (hole) creation time in NBTI stress. τ_1 , τ_2 , and τ_3 are the 1st, the 2nd, and the 3rd trapped hole creation times, respectively, in a device. The three $\log(\tau)$ distributions have a similar shape but are shifted by an amount $n\log(i)$.

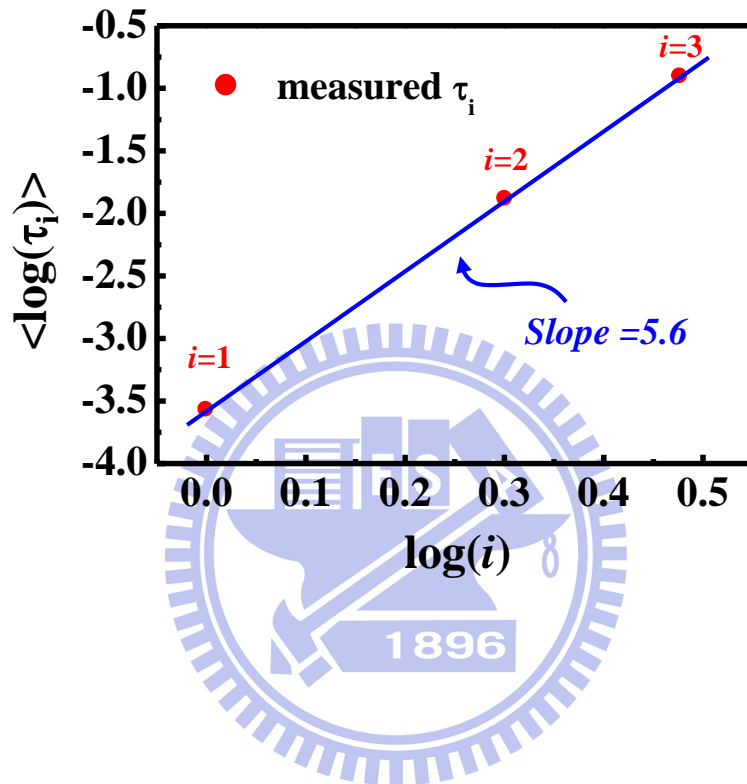


Fig. 2.9 We calculate the mean ($\langle \log(\tau_i) \rangle$) of the three $\log(\tau_i)$ distributions and reveal a relationship $\langle \log(\tau_i) \rangle - \langle \log(\tau_1) \rangle \sim n \log(i)$. i is a sequence number in trapped charge creation in NBTI stress and n is about 5.6.

trapped hole creation time	τ_1	τ_2	τ_3
mean of $\log(\tau)$ ($\langle \log(\tau) \rangle$)	-3.572	-1.885	-0.906
standard deviation of $\log(\tau)$	1.436	1.379	1.282

Table I The mean ($\langle \log(\tau_i) \rangle$) and the standard deviation of the three $\log(\tau_i)$ distributions. i is a sequence number in trapped charge creation in NBTI stress.

Chapter 3

Modeling of an NBTI induced ΔV_t Distribution

3.1 Preface

An NBTI induced ΔV_t distribution in pMOSFETs is explored and characterized. In the previous chapter, we characterize individual trapped charge creation by NBTI stress in a large number of nanoscale high-k pMOSFETs. The time constant (τ_i) distributions of the first three trapped holes ($i=1,2,3$) are obtained. The mean and the variance of the $\log(\tau_i)$ are investigated. We find that the characteristic times of a trapped charge creation scatter over several decades of time in nanoscale pMOSFETs, which is attributed to the dispersion from different local chemistry in reaction-diffusion (RD) model and 3D electrostatics such as random dopants and edge effects in a nanoscale device. Two NBTI degradation models, a RD model [10] and a charge trapping model [11-12], have been proposed. Since in this work our measured NBTI induced V_t degradation obeys a $t^{1/n}$ dependence, an NBTI induced ΔV_t distribution model will be developed based on the RD model.

We collect the first three trapped charge creation times (τ_i , $i=1,2,3$) from about 130 devices. A statistical model for an NBTI induced ΔV_t distribution by employing the RD model and convolving collected the trapped charge creation times (τ_i) and a single trapped charge induced V_t shift is developed. Our model reproduces measurement results of an overall NBTI induced ΔV_t distribution and its stress time evolutions well.

3.2 Reaction-Diffusion Model (RD Model)

According to the RD model, the stress time dependence of the number of NBTI generated traps in a device is shown below [10],

$$N_i = A \exp\left(\frac{2\gamma F}{3}\right) \exp\left(\frac{-E_D}{k_B T}\right) t^n, \quad n \sim 6, \quad \text{Eq. (3.1)}$$

and

$$A \equiv WLD_0^{1/6} \left[\frac{K_{F0} [SiH][h^+]}{pK_{R0}} \right]^{2/3}. \quad \text{Eq. (3.2)}$$

N_i is a total number of NBTI trapped charges in a device (also interpreted as a sequence number of the last created trapped charge). W is a gate width, L is a gate length, and other variables have their usual definitions in [10]. Three activation energies (E_F , E_R , $E_{diffusion}$) associated with K_F , K_R , and D in the RD model are lumped together and activation energy (E_D) in Eq. (3.1) is defined as

$$E_D = \frac{1}{6} E_{diffusion} + \frac{2}{3} (E_F - E_R). \quad \text{Eq. (3.3)}$$

By re-arranging the terms in Eq. (3.1), the i -th trapped charge creation time (τ_i) is shown below

$$\log(i) = \frac{1}{n} \log(\tau_i) + \frac{1}{2.3} \left(\frac{2\gamma F}{3} - \frac{E_D}{k_B T} \right) + \log(A). \quad \text{Eq. (3.4)}$$

3.3 Relationship of τ_i Distributions in Trapped Charge Creation

In the following, we re-arranging the terms and taking average in Eq. (3.4) and the relationship of the mean of the $\log(\tau_i)$ is obtained,

$$\langle \log(\tau_i) \rangle - \langle \log(\tau_1) \rangle = n \log(i). \quad \text{Eq. (3.5)}$$

It should be remarked that a real subtracted amount is 1.69 for $\log(\tau_2)$ (cf. $6\log(2)=1.81$) and 2.67 for $\log(\tau_3)$ (cf. $6\log(3)=2.86$). The slight difference is in that Eq. (3.5) is derived based on an NBTI evolution rate ($t^{1/n}$) with $n=6$ while our measured n is about 5.6 in an initial stress stage. Thus, we obtain $\langle \log(\tau_2) \rangle - \langle \log(\tau_1) \rangle = 5.6\log(2)=1.69$ and $\langle \log(\tau_3) \rangle - \langle \log(\tau_1) \rangle = 5.6\log(3)=2.67$. The calculated result from Eq. (3.5) is in reasonable agreement with the measurement result in [Table I](#).

Furthermore, we can shift the measured $\log(\tau_i)$ distribution by subtracting a term $n\log(i)$ from Eq. (3.5). The $\log(\tau_i) - n\log(i)$ distributions from the τ_1 , τ_2 , and τ_3 , respectively, are shown in [Fig. 3.1](#). A reasonably good match of the $\log(\tau)$ distributions from the τ_1 , τ_2 , and τ_3 is obtained. The solid line in [Fig. 3.1](#) represents a Gaussian-distribution fit. The standard deviation of the Gaussian distribution is about 1.6.

3.4 NBTI Stress Induced ΔV_t Spread

We measure threshold voltage shifts at different stress times in a number of

NBTI stressed pMOSFETs. The number of trapped holes and a total threshold voltage shift (ΔV_t) in each device are recorded. Fig. 3.2 shows the measurement results at a stress time of 0.01s, 1s and 100s, respectively. The y-axis is a total ΔV_t in stress and the x-axis is the number of trapped holes. Each data point represents a device. A straight line with a slope of 3.3mV, i.e., an average single-charge induced V_t shift, is drawn in the figure as a reference. The measurement data scatter along the lines. The ΔV_t and the number distributions broaden with stress time.

We extract the mean and the variance of the ΔV_t distributions. An average of ΔV_t in 130 devices is plotted in Fig. 3.3. The mean follows a power law dependence on stress time ($t^{1/n}$) in five decades of time with n about 6. The variance of the ΔV_t distribution also increases with stress time, as shown in Fig. 3.4. In our earlier work, we reported a two-stage V_t degradation by BTI stress [11]. The first stage is ascribed to the charging of pre-existing high-k dielectric traps and exhibits a $\log(t)$ dependence. The second stage degradation is caused by high-k dielectric trap creation and follows a power law dependence on stress time. Note that a $\log(t)$ degradation stage is not observed in this work possibly because of no many pre-existing traps in the current samples.

3.5 Monte Carlo Simulation Results and Discussion

A statistical model based on a Monte Carlo (MC) approach is developed. Based on the collected the trapped charge creation times (τ_i) and ΔV_t distributions, a Monte Carlo simulation can calculate the number of traps (N) and entire ΔV_t distributions. A Monte Carlo flowchart is shown in Fig. 3.5. In our MC simulation, a trapped charge creation sequence number (i) is assigned to each precursor in a device. The trapped

charge creation times (τ_i) of each precursor is chosen according to the Gaussian distribution in Fig. 3.1. A Poisson-distributed precursor number (M) in each device is assumed with a mean value of 24 in an 80nm×30nm device, which corresponds to a precursor density of 10^{12} cm^{-2} [30]. Each trapped charge creation time (τ_i) is then shifted according to Eq. (3.5). A trapped charge creation time with the shortest τ has $i = 1$, and the second shortest one has $i = 2$ and so on. In this approach, we can reproduce the same τ_i distributions (Fig. 3.6).

For a stress time t , the number of trapped charges N is computed by counting all the precursors with τ_i ($i=1,2,\dots,M$) less than t . For each counted trapped charge, a single trapped charge induced V_t shift (Δv_t) is randomly selected based on an exponential distribution, $f(|\Delta v_t|) = \exp(-|\Delta v_t|/\sigma_{amp})/\sigma_{amp}$, with $\sigma_{amp}=3.3\text{mV}$. An NBTI induced ΔV_t at a stress time t can be computed by summing up all the Δv_t , i.e., $\Delta V_t = \sum_{i=1}^N \Delta v_{t,i}$. In total, 5×10^5 devices are simulated in Monte Carlo simulation. The mean and the variance of the simulated ΔV_t distributions versus stress time are shown in Fig. 3.3 and Fig. 3.4, respectively. Good agreement between the Monte Carlo simulation and measurement results is obtained. In addition, we compare measured and simulated ΔV_t distributions at different stress times. Complementary cumulative distribution functions (1-CDF) of NBTI induced ΔV_t at a stress time of $t=0.01\text{s}$, 1s and 100s are plotted in Fig. 3.7. The inset of the figure is the probability density function of ΔV_t . Our simulation is in good agreement with measurement results.

Finally, we also compare this model with the Poisson distributed trap number model [17-19] at a stress time of 100s. To examine the difference in a ΔV_t distribution tail, complementary cumulative distribution functions (1-CDF) of the two models at a

stress time of 100s are plotted in Fig. 3.8 with a logarithmic scale in y-axis. The probability density distributions of a trapped charge number from the two models are plotted in Fig. 3.9. The Poisson model apparently yields a broader distribution in trapped charge number (N) and thus a larger NBTI induced ΔV_t tail. The difference between the two models increases with stress time as more trapped charges are created. The reason is that individual trapped charge creations are un-correlated in the Poisson model. In other words, each new trap creation in a device has the same probability regardless of how many traps have been created. Nevertheless, the RD model and measurement results show that NBTI degradation obeys a power-law ($t^{1/n}$) dependence on stress time, implying that trapped charge creation becomes more difficult as a sequence number of charge creation increases. We also compare NBTI failure rates in 100sec stress from the two models with two ΔV_t failure criteria, $\Delta V_t > 50\text{mV}$ and 100mV (Table II). The difference between the two models increases as a failure ΔV_t increases. Our model can fit an NBTI distribution tail better.

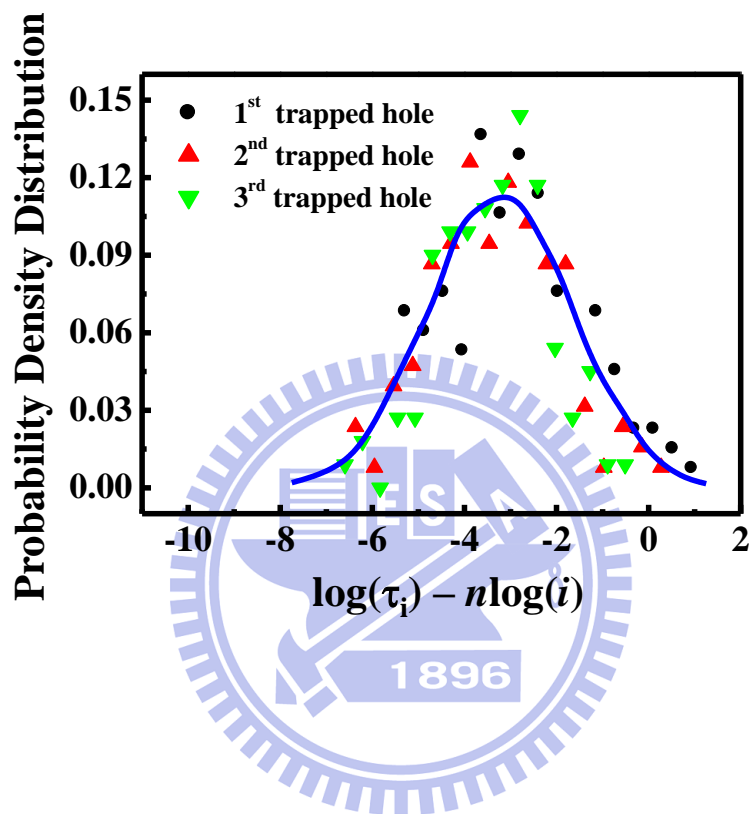


Fig. 3.1 The probability density distributions of $\log(\tau_i) - n \log(i)$. The solid line represents a Gaussian-distribution fit.

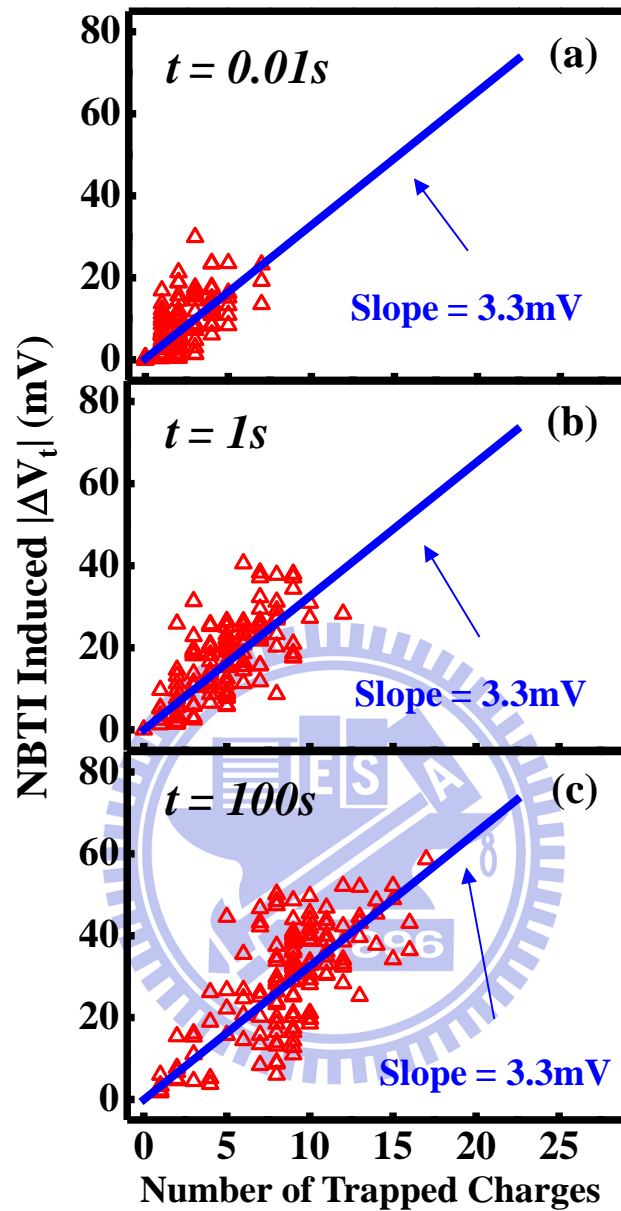


Fig. 3.2 NBTI induced ΔV_t versus number of created trapped holes in a device at a stress time of 0.01s (a), 1s (b) and 100s (c). Each data point represents a device. A straight line with a slope of 3.3 mV is drawn as a reference.

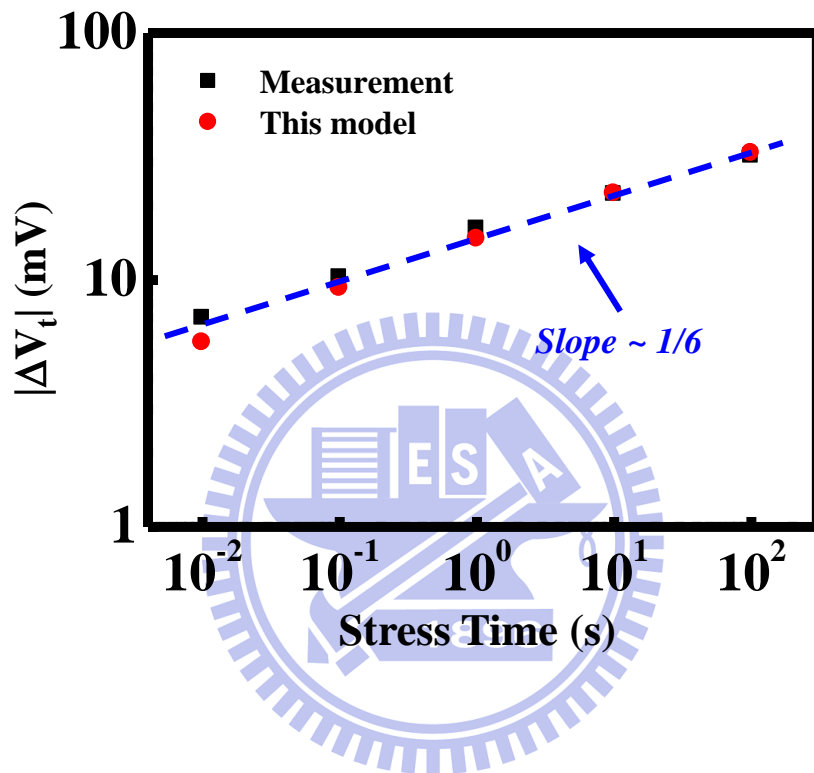


Fig. 3.3 The mean of the ΔV_t distribution versus NBTI stress time from measurement and from our model.

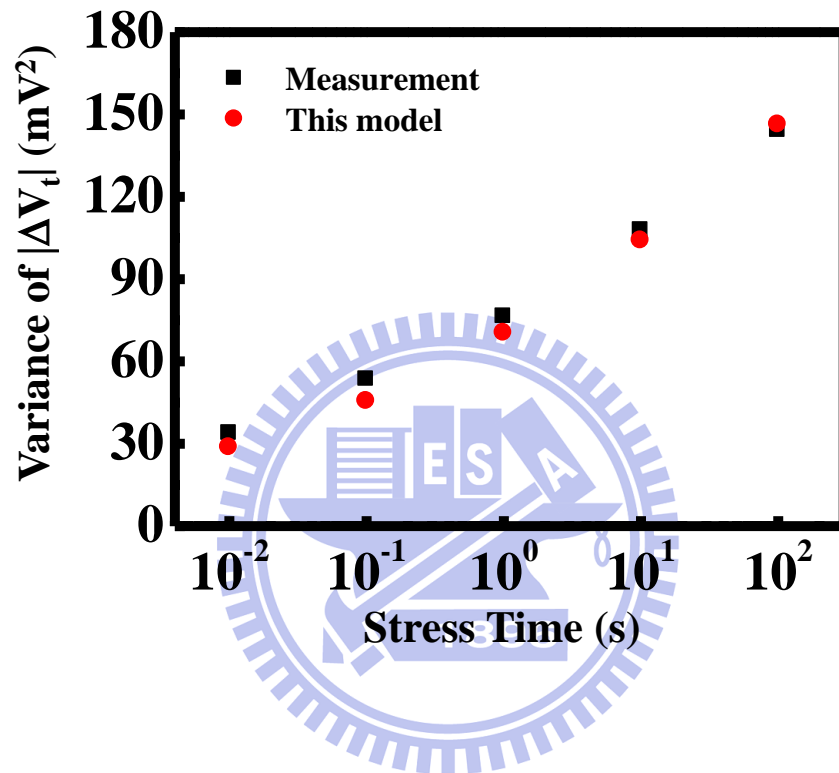


Fig. 3.4 The variance of the ΔV_t distribution versus NBTI stress time from measurement and from our model.

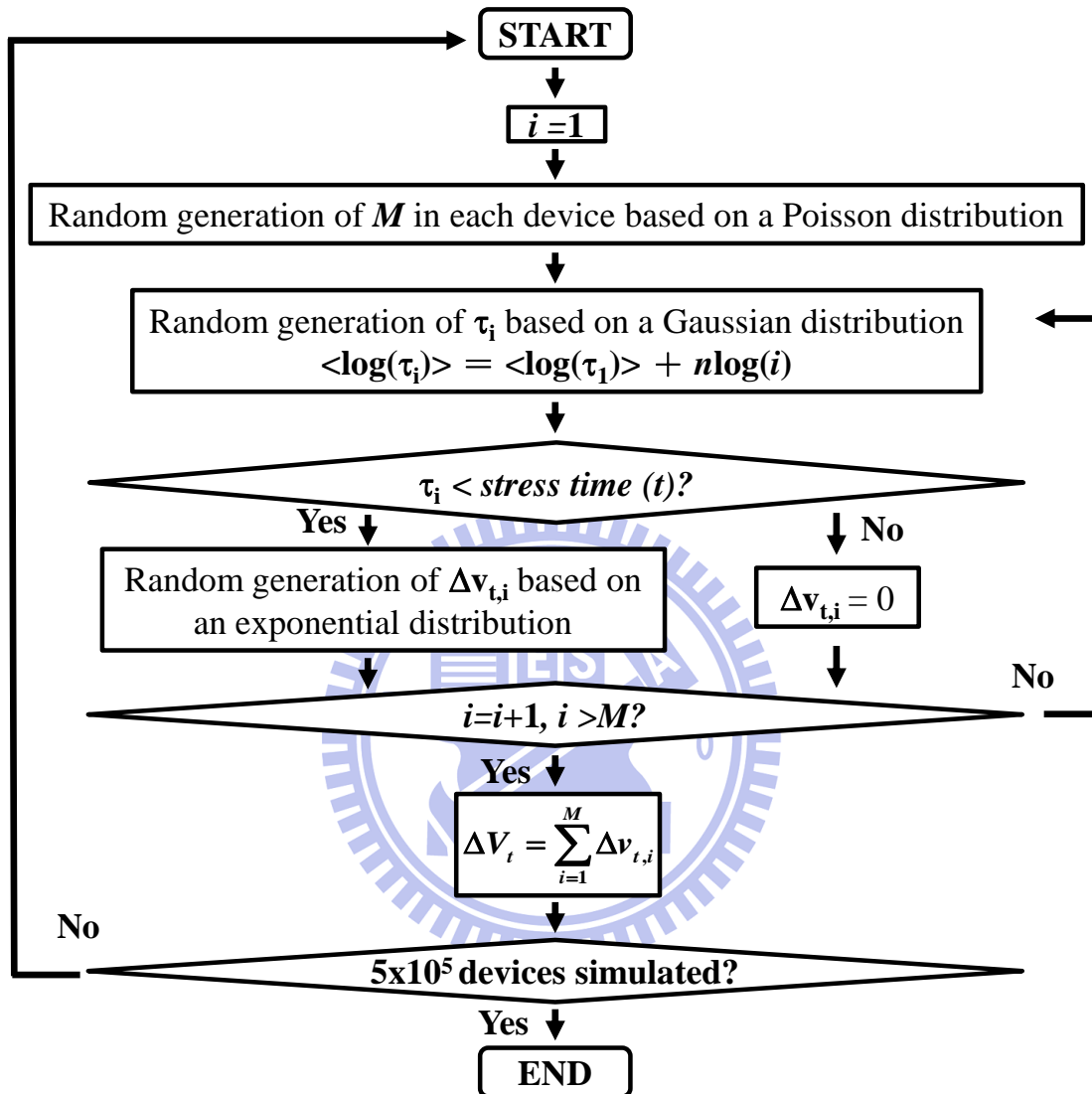


Fig. 3.5 A Monte Carlo simulation flowchart. M is the number of precursors in a device. A precursor density of 1×10^{12} $1/\text{cm}^2$ is assumed.

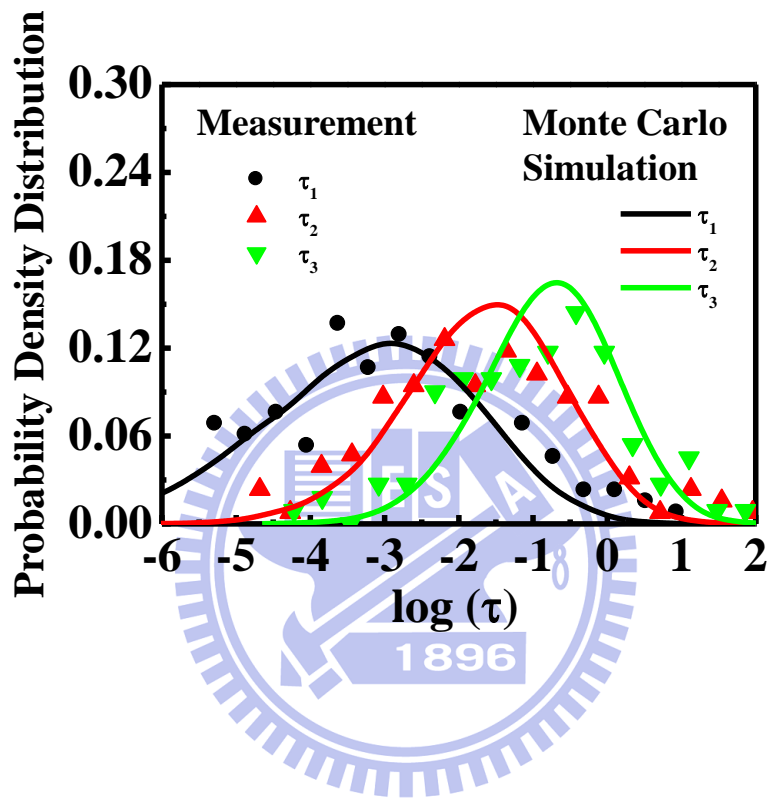


Fig. 3.6 Probability density distributions of a trapped charge (hole) creation time in a $\log(\tau)$ scale. The symbols are measurement result and the solid lines are from Monte Carlo simulation.

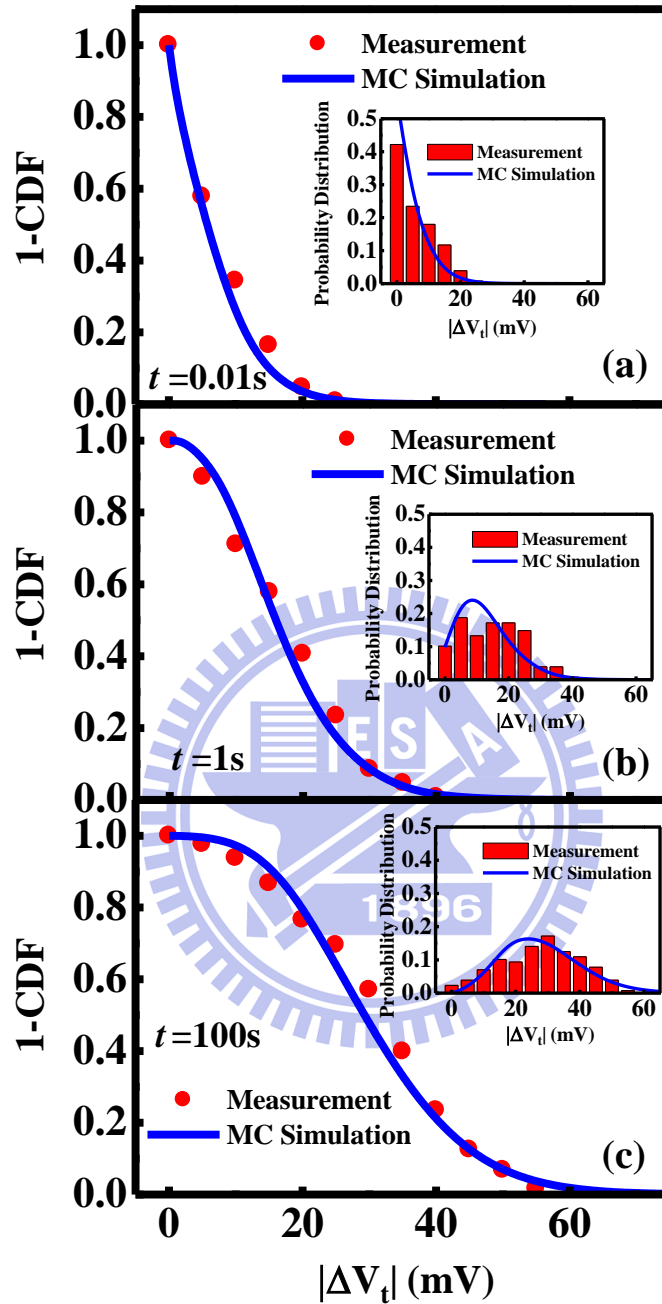


Fig. 3.7 Complementary cumulative distribution functions (1-CDF) of NBTI induced ΔV_t from measurement and from a Monte Carlo simulation. The stress time is 0.01s (a), 1s (b) and 100s (c), respectively. The inset shows the probability distributions of ΔV_t .

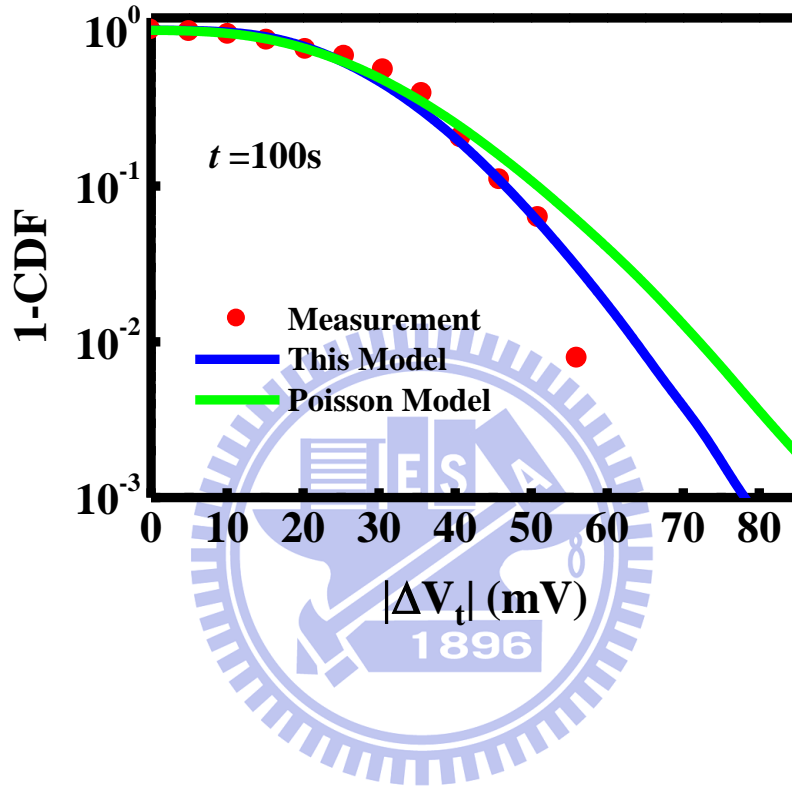


Fig. 3.8 Comparison of NBTI induced ΔV_t distributions (1-CDF) calculated from this model and from the Poisson distributed trap number model. The dots are measurement result. The stress time is 100s.

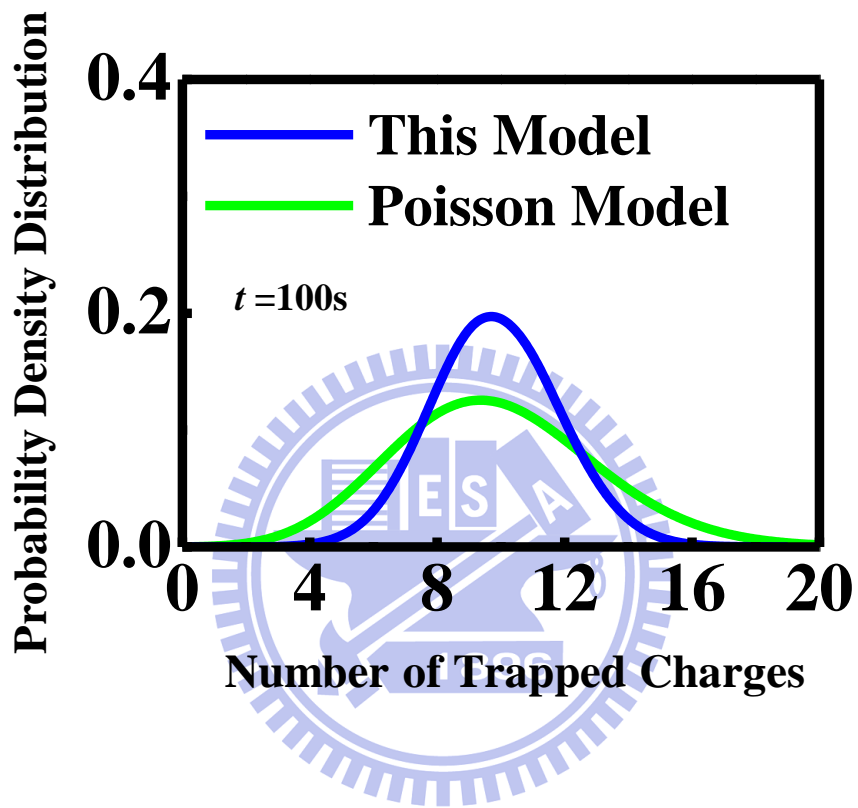


Fig. 3.9 The probability density distributions of a trapped charge number from our model and from the Poisson distributed trap number model.

NBTI Failure Criterion	Poisson Model	This Model	Measurement
$\Delta V_t = 50\text{mV}$	10.98%	7.62%	9 / 132
$\Delta V_t = 100\text{mV}$	0.032%	0.003%	N / A

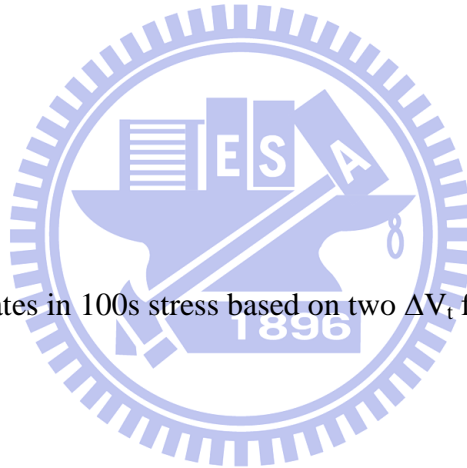


Table II NBTI failure rates in 100s stress based on two ΔV_t failure criteria.

Chapter 4

Conclusion

A discrete feature in NBTI stress V_t evolutions due to individual trapped charge creations in small-area devices is observed. Single charge creation times and induced V_t shifts are clearly defined. This single charge characterization approach allows us to gain insight into NBTI induced threshold voltage shift distributions in small-area devices. Statistical characterization of individual trapped charge creations in NBTI stress in a large number of nanoscale high-k (HfSiON)/metal gate (TiN) pMOSFETs is performed and an NBTI induced ΔV_t distribution have been investigated.

Two factors are found to influence an NBTI induced ΔV_t distribution. One is the dispersion of single trapped charge induced threshold voltage shift and the other one is the dispersion of trapped charge creation times. The broad distribution of trapped charge creation times is attributed to the dispersion from different local chemistry and 3D electrostatics such as random dopants and edge effects in a nanoscale device.

We develop a statistical model based on measured trap characteristic time distributions to simulate an NBTI induced ΔV_t distribution in nanoscale devices. A correlation between the trapped charge creation distributions and the spread of an NBTI induced ΔV_t distribution has been established. Our model can reproduce a measurement result of an NBTI induced ΔV_t distribution and its stress time evolution well.

Reference

- [1] S. Pae, J. Maiz, C. Prasad, and B. Woolery, "Effect of BTI Degradation on Transistor Variability in Advanced Semiconductor Technologies," *IEEE Trans. Device Mater. Rel.*, vol. 8, no. 3, pp. 519-525, 2008.
- [2] S. E. Rauch, "Review and Reexamination of Reliability Effects Related to NBTI-Induced Statistical Variations," *IEEE Trans. Device Mater. Rel.*, vol. 7, no. 4, pp. 524-530, 2007.
- [3] J. P. Chiu, Y. T. Chung, Tahui Wang, Min-Cheng Chen, C. Y. Lu, and K. F. Yu, "A Comparative Study of NBTI and RTN Amplitude Distributions in High- κ Gate Dielectric pMOSFETs," *IEEE Electron Device Lett.*, vol. 33, no. 2, pp. 176-178, 2012.
- [4] S. Zafar, Y. H. Kim, V. Narayanan, C. Cabral Jr., V. Paruchuri, B. Doris, J. Stathis, A. Callegari and M. Chudzik, "A Comparative Study of NBTI and PBTI (Charge Trapping) in SiO₂/HfO₂ Stacks with FUSI, TiN, Re Gates," in *VLSI Symp. Tech. Dig.*, pp. 23-25, 2006.
- [5] S. Zafar, A. Kumar, E. Gusev and E. Cartier, "Threshold Voltage Instabilities in High-k Gate Dielectric Stacks," *IEEE Trans. Device Mater. Rel.*, vol. 5, pp. 45-64, 2005.
- [6] V. Reddy, A.T. Krishnan, A. Marshall, J. Rodriguez, S. Natarajan, T. Rost, and S. Krishnan, "Impact of Negative Bias Temperature Instability on Digital Circuit Reliability," in *Proc. Int. Reliab. Phys. Symp.*, pp. 248-254, 2002.
- [7] A. T. Krishnan, V. Reddy, D. Aldrich, J. Raval, K. Christensen, J. Rosal, C. O'Brien, R. Khamankar, A. Marshall, W-K. Loh, R. McKee, S. Krishnan, "SRAM Cell Static Noise Margin and V_{MIN} Sensitivity to Transistor Degradation," in *IEDM Tech. Dig.*, pp. 1-4, 2006.

- [8] M. Agostinelli, S. Lau, S. Pae, P. Marzolf, H. Muthali, and S. Jacobs, "PMOS NBTI-induced circuit mismatch in advanced technologies," in *Microelectron. Reliab.*, vol. 46, pp. 63-68, 2006.
- [9] N. K. Jha, P. S. Reddy, D. K. Sharma, and V. R. Rao, "NBTI Degradation and Its Impact for Analog Circuit Reliability," *IEEE Trans. Electron Devices*, vol. 52, no. 12, pp. 2609-2615, 2005.
- [10] A. E. Islam, H. Kufluoglu, D. Varghese, S. Mahapatra, and M. A. Alam, "Recent Issues in Negative-Bias Temperature Instability: Initial Degradation, Field Dependence of Interface Trap Generation, Hole Trapping Effects, and Relaxation," *IEEE Trans. Electron Devices*, vol. 54, no. 9, pp. 2143-2154, 2007.
- [11] C. T. Chan, C. J. Tang, T. Wang, H. C.-H. Wang, and D. D. Tang, "Positive Bias and Temperature Stress Induced Two-Stage Drain Current Degradation in HfSiON nMOSFET's," in *IEDM Tech. Dig.*, pp. 571-574, 2005.
- [12] T. Grasser, B. Kaczer, W. Goes, H. Reisinger, T. Aichinger, P. Hehenberger, P.-J. Wagner, F. Schanovsky, J. Franco, M. Toledano, and M. Nelhiebel, "The Paradigm Shift in Understanding the Bias Temperature Instability : From Reaction-Diffusion to Switching Oxide Traps," *IEEE Trans. Electron Devices*, vol. 58, no. 11, pp. 3652-3665, 2011.
- [13] K. O. Jeppson and C. M. Svensson, "Negative bias stress of MOS devices at high electric fields and degradation of MNOS devices," *J. Appl. Phys.*, vol. 48, no. 5, pp. 2004-2014, 1977.
- [14] S. Ogawa and N. Shiono, "Generalized diffusion-reaction model for the low-field charge build up instability at the Si-SiO₂ interface," *Phys. Rev. B*, vol. 51, no. 7, pp. 4218-4230, 1995.
- [15] M. A. Alam, "A critical examination of the mechanics of dynamic NBTI for

- PMOSFETs,” in *IEDM Tech. Dig.*, pp. 345-348, 2003.
- [16] Jung-Piao Chiu, Chi-Wei Li, and Tahui Wang, “Characterization and modeling of trap number and creation time distributions under negative-bias-temperature stress,” *Appl. Phys. Lett.*, vol. 101, no. 8, p. 082906, 2012.
- [17] B. Kaczer, T. Grasser, Ph. J. Roussel, J. Franco, R. Degraeve, L.-A. Ragnarsson, E. Simoen, G. Groeseneken, and H. Reisinger, “Origin of NBTI Variability in Deeply Scaled pFRTs,” in *Proc. Int. Reliab. Phys. Symp.*, pp. 26-32, 2010.
- [18] B. Kaczer, Ph. J. Roussel, and T. Grasser, “Statistics of Multiple Trapped Charges in the Gate Oxide of Deeply Scaled MOSFET Devices—Application to NBTI,” *IEEE Electron Device Lett.*, vol. 31, no. 5, pp. 411-413, 2010.
- [19] M. Toledano-Luque, B. Kaczer, J. Franco, P. J. Roussel, T. Grasser, T. Y. Hoffmann, and G. Groeseneken, “From mean values to distributions of BTI lifetime of deeply scaled FETs through atomistic understanding of the degradation,” in *VLSI Symp. Tech. Dig.*, pp. 152-153, 2011.
- [20] H. Reisinger, O. Blank, W. Heinrigs, A. Muhlhoff, W. Gustin and C. Schlunder, “Analysis of NBTI Degradation- and Recovery-Behavior Based on Ultra-Fast V_T -Measurements”, in *Proc. Int. Reliab. Phys. Symp.*, pp. 448-453, 2006.
- [21] C. Shen, M. -F. Li, X. P. Wang, Y. -C. Yeo, and D. -L. Kwong, “Fast Measurement Technique of MOSFET I_d - V_g Characteristics,” *IEEE Electron Device Lett.*, vol. 27, no. 1, pp. 55-57, 2006.
- [22] T. Wang, C. T. Chan, C. J. Tang, C. W. Tsai, H. C. -H. Wang, M. H. Chi and D. D. Tang, “A Novel Transient Characterization Technique to Investigate Trap Properties in HfSiON Gate Dielectric MOSFETs — From Single Electron Emission to PBTI Recovery Transient,” *IEEE Trans. Electron Devices*, vol. 53, pp. 1073-1079, 2006.

- [23] C. T. Chan, C. J. Tang, C. H. Kuo, H. C. Ma, C. W. Tsai, H. C. H. Wang, M. H. Chi, and Tahui Wang, "Single-Electron Emission of Traps in HfSiON as High-k Gate Dielectric for MOSFETs", in *Proc. Int. Reliab. Phys. Symp.*, pp. 41-44, 2005.
- [24] C. T. Chan, H. C. Ma, C. J. Tang and T. Wang, "Investigation of Post-NBTI Stress Recovery in pMOSFETs by Direct Measurement of Single Oxide Charge De-Trapping," in *VLSI Symp. Tech. Dig.*, pp. 90-91, 2005.
- [25] J. P. Chiu, Y. H. Liu, H. D. Hsieh, C. W. Li, M. C. Chen and Tahui Wang, "Statistical Characterization and Modeling of the Temporal Evolutions of ΔV_t Distribution in NBTI Recovery in Nanometer MOSFETs," *IEEE Trans. Electron Devices*, vol. 60, pp. 978-984, 2013.
- [26] T. Grasser, H. Reisinger, P.-J. Wagner, W. Goes, F. Schanovsky and B. Kaczer, "The Time Dependent Defect Spectroscopy (TDDS) Technique for the Bias Temperature Instability," in *Proc. Int. Reliab. Phys. Symp.*, pp. 16-25, 2010.
- [27] C. T. Chan, C. J. Tang, T. Wang, H. C. -H. Wang, and D. D. Tang, "Characteristics and Physical Mechanisms of Positive Bias and Temperature Stress-Induced Drain Current Degradation in HfSiON nMOSFETs," *IEEE Trans. Electron Devices*, vol. 53, no. 6, pp. 1340-1346, 2006.
- [28] A. Asenov, R. Balasubramaniam, A. R. Brown and J. H. Davies, "RTS Amplitudes in Decanometer MOSFETs: 3-D Simulation Study," *IEEE Trans. Electron Devices*, vol. 50, no.3, pp. 839-845, 2003.
- [29] S. Amoroso, L. Gerrer, S. Markov, F. Adamu-Lema, and A. Asenov, "Comprehensive statistical comparison of RTN and BTI in deeply scaled MOSFETs by means of 3D 'atomistic' simulation," in *Proc. Eur. Solid-State Device Res. Conf.*, pp. 109-112, 2012.
- [30] A. Stesmans, "Dissociation kinetics of hydrogen-passivated P_b defects at the (111)

Si/SiO₂ interface,” *Phys. Rev. B*, vol. 61, no. 12, pp. 8393-8403, 2000.



簡 歷

姓名：李啟偉

性別：男

生日：民國 78 年 2 月 14 日

籍貫：台灣省嘉義市

地址：嘉義市西區文化里 2 鄰康樂街 105 號之 1 六樓 2

學歷：國立交通大學 電子工程學系 96.9-100.6

國立交通大學電子工程研究所碩士班 100.9-102.7

碩士論文題目：

高介電係數閘極電晶體之負偏壓溫度不穩定
性引致臨界電壓改變量分佈之統計特性和模
式

**Statistical Characterization and Modeling of
NBTI Induced ΔV_t Distribution in High-k Gate
Dielectric pMOSFETs**